UDC 533.6.013.422
533.6.011.5

# TECHNICAL REPORT OF NATIONAL AEROSPACE LABORATORY

## TR-125T

## Experimental and Calculated Results of Supersonic Flutter Characteristics of a Low Aspect-Ratio Flat-Plate Surface

Eiichi NAKAI · Toshiro TAKAGI

Koji ISOGAI · Toshiyuki MORITA

January 1967

**NATIONAL AEROSPACE LABORATORY**

CHŌFU, TOKYO, JAPAN

## List of NAL Technical Reports

| | | | |
|---|---|---|---|
| TR–95 | A Few Comments on the Longitudinal Handling Qualities of Airplanes | Hiroshi ARAKI | Nov. 1965 |
| TR–96T | A Generalized Functional Formalism for Turbulence | Iwao HOSOKAWA | Dec. 1965 |
| TR–97 | A Theoretical of the Compressible Flow Through the Axial Turbo-Machines (I) —Non-Swirling Fluids in Ducts— | Shōichi FUJII | Dec. 1965 |
| TR–98 | Some Effects of Taper Ratio on the Transonic Flutter Characteristics of a Series of Thin Cantilever Wings Having a Sweptback Angle of 45° and an Aspect Ratio 4.0 | Eiichi NAKAI, Toshiro TAKAGI & Yasukatsu ANDO | Dec. 1965 |
| TR–99 | A Study of Dial Legibility | Noriko MIYOSHI, Masanori OKABE & Sumiko ISHIKAWA | Feb. 1966 |
| TR–100 | Linearized Aerodynamic Theory of Rotor Bladed (III) —Method for Solving Lifting-Equations— | Teruo ICHIKAWA | Feb. 1966 |
| TR–101 | Meteorological Conditions on Aircraft Icing (I) | Syōzi KOSHEKI, Kiiti TADERA, Hideo IZUMI, Mikio ŌTA & Masakatu MINEGISI | Feb. 1966 |
| TR–102 | An Approximate Calenlation for Supersonic Flow Past Bodies of Rocket Vehicles (II) —Linearized Flow with Attack Angle— | Takashi TANI | Mar. 1966 |
| TR–103T | Basic Considerations for Treating Non-Equilibrium Fluids —A Functional Approach to Non-Equilibrium Statistical Mechanics— | Iwao HOSOKAWA | Mar. 1966 |
| TR–104 | The Camber Distribution of a Spanwise Uniformly Loaded Subsonic Wing | Toshio KAWASHAKI & Mashao EBIHARA | Apr. 1966 |
| TR–105 | A Psychological Study on the Mental Stress of Piloto (I) —Pules and Respiratory rate during flight— | Noriko MIYOSHI, Moriyuki MOMONA & Mashanori OKABE | Apr. 1966 |
| TR–106 | On Reversal of Effectiveness of Control Surfaces in Transonic Flow | Nobuhiko KAMIYA & Shinsaku SEGAWA | May 1966 |
| TR–107 | Ionized Flow in a Conical Shock Tube | Riiti MATSUZAKI | May 1966 |
| TR–108 | Some High-Speed Tests on Impules Turbine Cascades | Hiroshi KONDŌ, Mitsuhiro MINODA, Norio YAMAZAKI & Noboru HURUKAWA | June 1966 |
| TR–109 | A Study on the Large-Scale Air Ejector | Shōichi FUJII, Mitsuo GOMI & Noboru SUGAHARA | July 1966 |
| TR–110 | Some Investigations on Inviscid Boundary Layer of Magneto-hydrodynamics | Kenji INOUE | Aug. 1966 |
| TR–111T | An Asymptotic Solution of the Nonlinear Equations of Motion of an Airplane | Hiroshi ENDŌ | Aug. 1966 |
| TR–112 | A Theoretical Investigation of the Compressible Flow Trough the Axial Turbo-Machines (II) —Swirling Fluids— | Shoichi FUJII | Aug. 1966 |
| TR–113 | Experimental Study on the Ground Effect of a Model Helicopter Rotor in Hovering | Jiro KŌO & Tōichi OKA | Aug. 1966 |

# Experimental and Calculated Results of Supersonic Flutter Characteristics of a Low Aspect-Ratio Flat-Plate Surfaces*

By

Eiichi NAKAI**, Toshiro TAKAGI**, Koji ISOGAI**, and Toshiyuki MORITA**

## SUMMARY

An experimental investigation of the supersonic flutter characteristics of thin cantilever plate surfaces having a plate aspect-ratio of 1.0 and a taper ratio of 0.63 has been conducted in the N.A.L. 1 m×1 m supersonic blow-down wind tunnel at Mach numbers from 1.519 to 4.140. Each model was cantilevered on the side wall of test section of the wind tunnel with a model injection-rejection rig.

The experimental results were compared with the calculated results employing piston theory and quasi-steady second-order theory as the required oscillatory aerodynamic forces and utilizing the first three normal coupled modes which include cambering deflections. Both theories were unconservative for the cofiguration of the models experimented and the range of Mach numbers investigated.

## INTRODUCTION

Although some works of experimental investigation of the supersonic flutter characteristics of low aspect-ratio surfaces have been done, i.e., refs. 1 through 4, almost all of them are up to Mach number 3.0 and the intervals of Mach numbers investigated are rather wide, and also data was unavailable for the plan form of the surfaces experimented, which is identical to that of the wings of "NAL-16" research rocket (reference 5). There was a need for more information of the supersonic flutter characteristics of the configuration, both to provide the data for design criteria and to provide a basis for comparison of theory and experiment extending Mach number up to around 4.0.

The semi-span models of twelve different sizes of a same plan form, keeping the thickness of the surfaces constant, were constructed, and flutter data were compared with theoretical calculations with the use of theory of reference 6 based on piston theory for the full range of Mach numbers experimented and quasi-steady second-order theory for Mach numbers under 2.5. Mode shapes of the model used in the computation were experimentally determined by the method of reference 7.

## SYMBOLS

| | |
|---|---|
| $A$ | panela spect ratio (semispan$^2$/ panel area) |
| $A_{ij}, B_{ij}, C_{ij}, D_{ij}$ | surface integrals of wing properties |
| $a$ | speed of sound |
| $\left(a_i^{(n)}\right)_p$ | coefficients of polynomials approximating mode shape at station $n$ in mode $i$ |
| $b$ | local semi-chord |

* Received 17th December, 1966
** The First Airframe Division

$\frac{b_R \omega_\alpha}{a}\sqrt{\mu}$ stiffness-altitude parameter

$c$ local chord

$f_f$ flutter frequency

$f_i(x', y')$ modal function for mode $i$

$f_i^{(n)}(x)$ polynimial which approximatse mode $i$ at station $n$

$f_n$ natural frequency of $n$-th mode ($n$=1, 2, and 3)

$g$ structural damping coefficient

$I$ number of modes in analysis

$k$ reduced frequency, $b\omega/V$

$l$ length of semispan, measured normal to stream direction

$M$ Mach number

$M_i$ generalized mass for mode $i$

$m(x', y')$ mass per unit area

$m_0$ mass per unit area of flat plate surface

$N$ number of spanwise stations used to approximate wing properties

$P$ degree of polynomials

$p$ pressure

$q$ dynamic pressure

$t$ thickness

$t_\nu$ thickness terms defined by equation (10)

$V$ velocity

$W$ total weight of surface

$w$ downwash velocity

$X=\left(\frac{\omega_1}{\omega}\right)^2(1+ig)$

$x', y'$ Cartesian coordinates

$x, y$ coordinates along chord, in fraction of local chord, and along span, in fraction of semispan, respectively

$Z(x', y')$ function describing airfoil surface, positive away from mean surface

$Z^{(n)}(x)$ function describing airfoil contour at station $n$, positive away from airfoil mean line

$\beta=\sqrt{M^2-1}$

$\delta$ leading- and trailing-edge bevel, measured parpendicular to edges

$\mu=\frac{\text{Mass of wing}}{\pi\rho\int_0^t b^2 dy'}$ mass ratio

$\xi_i(t)$ generalized coordinate of motion in mode $i$

$\bar{\xi}_i$ amplitude of generalized coordinate for mode $i$

$\rho$ air density

$\omega_i$ $i$-th natural circular frequency

$\omega_\alpha$ wing torsional circular frequency

Subscripts:

$i, j$ indices indicating mode

$\infty$ free stream

$p, r$ indices pertaining to terms in polynomials

$R$ reference

$ex$ experimental

$th$ theoretical

Superscripts:

$1, 2, 3, \cdots n$ spanwise station

Matrix notation

$[\ ]$ square

$\begin{bmatrix} \searrow & \\ & \searrow \end{bmatrix}$ diagonal

## MODEL DESCRIPTION

The model configuration used in the investigation is shown in figure 1. With keeping the plate thickness constant, the size of the models was gradually varied from the full-size of the wing of "NAL-16" rocket to the scale of 65%, designated as "Model-100" and "Model-65" respectively, totaling the number of models constructed to twelve (as indicated in the column of "Model" of table 1), for the purpose of obtaining flutter points at the lower stagnation pressure during the operation of the wind tunnel for the respective Mach number

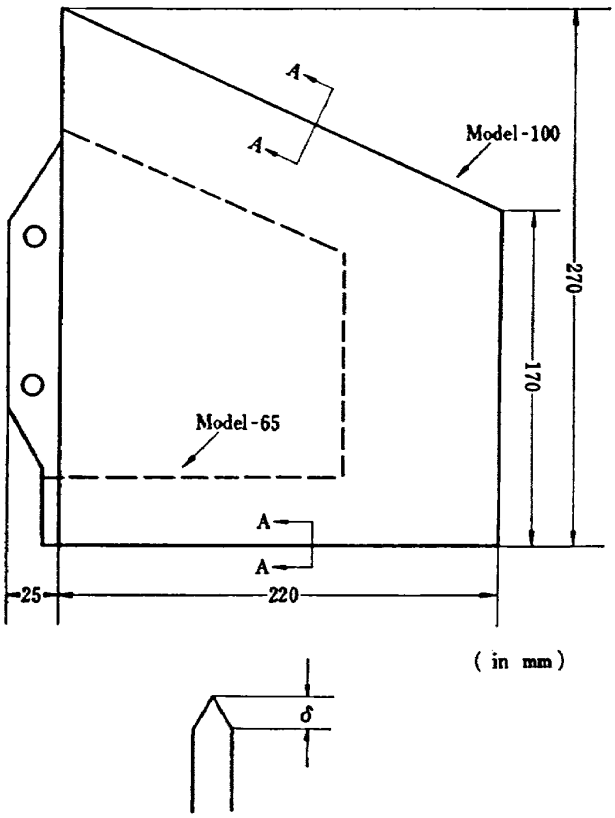


Section A-A

Fig. 1 Model Plan Form

experimented.

All models were made from magnesium sheets of 2 mm thickness with alminum alloy root. Leading and trailing edges were beveled with the angle of 60°, and the larger the model, the longer the length of the overhung part of the root chord, as shown in figure 1. The model was attached to the mounting block with two steel pins of 10 mm diameter. This method of attaching the model to the block was same as in the wings of "NAL-16" rocket. The model being attached to the model injection-rejection rig, was mounted on the side wall of the wind tunnel. By the use of the model injection-rejection rig, the breakage of the model was avoided during the starting- and stopping-shock passing through the test section of wind tunnel. The method of mounting the model in the injection-rejection rig is illustrated in figure 2.

## TEST APPARATUS AND INSTRUMENTATION

The tests were conducted in the N.A.L. 1 m×1 m supersonic blow-down wind tunnel (reference 8). This tunnel is of the intermittent type with flexible nozzle which facilitates to vary Mach numbers continuously from 1.5 to around 4.0, and operates from a high pressure air source to atmosphere.

Each model was instrumented with strain gages externally mounted on the wing near the root and oriented so as to distinguish between wing bending and torsion signals. The strain gages were used to provide an indication of the start of flutter and to obtain a record of the frequency of wing bending and torsion

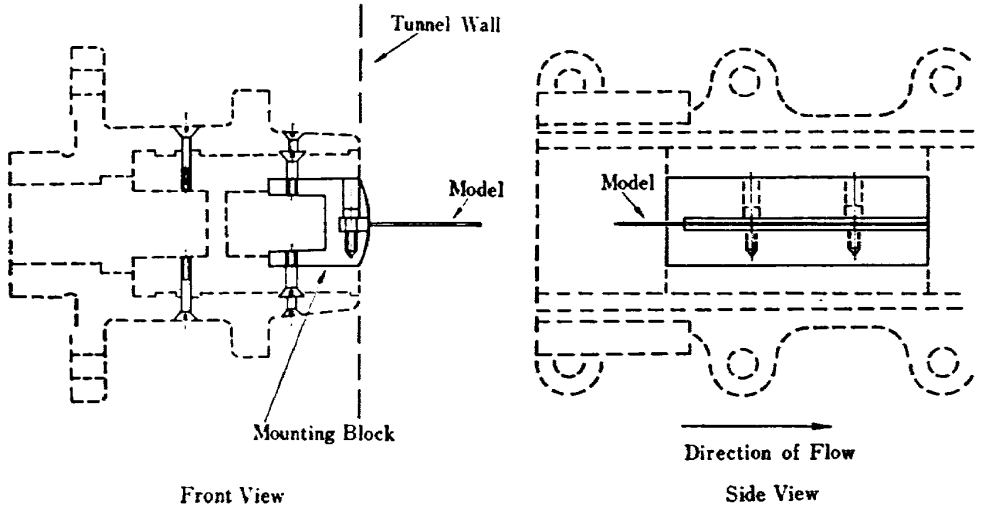


Fig. 2 Method of Mounting Model

oscillations.

During each test, continuous records of wind tunnel conditions, *i.e.*, stagnation pressure and temperature and test section static pressure, and model behavior were simultaneously recorded on self-balancing potentiometer recorders and a multichannel recording oscillograph, respectively.

A high-speed, 16 mm motion-picture camera (approximately 4,000 frames per second) was used to obtain a visual record of wing deflection during some of the flutter tests. These films served as an aid in defining the mode shape and magnitude of flutter.

## VIBRATION TEST

The natural frequencies and node lines of all models constructed were measured by the use of flutter model vibration rig shown in reference 9, and the structural damping coefficients of models were obtained from the records of natural damping oscillation, as indicated in table 1. The first three natural mode shapes

Table 1. Measured Frequencies, Flutter Frequencies and Structural Damping Coefficients.

| Model | Frequencies c.p.s. | | | | $M$ | Stract. Damp. Coeff. |
|---|---|---|---|---|---|---|
| | $f_1$ | $f_2$ | $f_3$ | $f_{f,ex}$ | | |
| 65* | 84.5 | 222.8 | 474.6 | | | |
| 70 | 72.5 | 193.1 | 410.5 | 125.0 | 1.527 | 0.0123 |
| 72.5 | 67.7 | 175.6 | 375.4 | 116.9<br>114.9 | 1.519<br>1.780 | 0.0121 |
| 75 | 63.7 | 167.6 | 354.9 | 108.7<br>111.1 | 1.771<br>2.037 | 0.0124 |
| 77.5 | 58.9 | 149.0 | 325.3 | 102.0<br>103.1 | 2.037<br>2.282 | 0.0105 |
| 80 | 54.9 | 141.3 | 296.8 | 96.1 | 2.528 | 0.0236 |
| 82.5 | 52.2 | 137.4 | 291.5 | 94.1<br>91.7 | 2.517<br>2.828 | 0.0165 |
| 85 | 48.9 | 120.8 | 264.1 | 84.7 | 3.064 | 0.0225 |
| 87.5 | 45.4 | 117.8 | 251.9 | 81.6<br>81.6<br>81.3 | 3.071<br>3.280<br>3.595 | 0.0152 |
| 90 | 43.9 | 110.0 | 238.5 | 76.9<br>76.9<br>76.3 | 3.583<br>3.848<br>4.140 | 0.0158 |
| 95* | 38.5 | 91.4 | 200.9 | | | |
| 100* | 33.9 | 86.4 | 182.2 | | | |

* No flutter was obtained.

Table 2. Representative Mode Shapes and Node Lines of Model.

| $x$ | Normalized Deflection at $y$ | | | | |
|---|---|---|---|---|---|
| | 0.2 | 0.4 | 0.6 | 0.8 | 1.0 |
| 1st Mode | | | | | |
| 0 | 0.072 | 0.210 | 0.389 | 0.617 | 0.884 |
| 0.2 | 0.078 | 0.219 | 0.421 | 0.661 | 0.915 |
| 0.4 | 0.085 | 0.239 | 0.459 | 0.697 | 0.950 |
| 0.6 | 0.092 | 0.251 | 0.486 | 0.732 | 0.976 |
| 0.8 | 0.095 | 0.263 | 0.500 | 0.747 | 0.990 |
| 1.0 | 0.099 | 0.270 | 0.507 | 0.753 | 1.000 |
| 2nd Mode | | | | | |
| 0 | 0.250 | 0.548 | 0.891 | 0.991 | 1.000 |
| 0.2 | 0.182 | 0.407 | 0.577 | 0.632 | 0.538 |
| 0.4 | 0.095 | 0.213 | 0.261 | 0.246 | 0.070 |
| 0.6 | 0.006 | −0.014 | −0.082 | −0.159 | −0.358 |
| 0.8 | −0.098 | −0.259 | −0.500 | −0.616 | −0.692 |
| 1.0 | −0.197 | −0.526 | −0.751 | −0.903 | −0.952 |
| 3rd Mode | | | | | |
| 0 | −0.446 | 0.773 | −0.619 | −0.142 | 0.787 |
| 0.2 | −0.311 | 0.526 | −0.345 | 0.187 | 0.919 |
| 0.4 | −0.207 | 0.316 | −0.121 | 0.302 | 1.000 |
| 0.6 | −0.207 | 0.329 | −0.194 | 0.199 | 0.837 |
| 0.8 | −0.265 | 0.469 | −0.408 | −0.058 | 0.578 |
| 1.0 | −0.331 | 0.657 | −0.619 | −0.349 | 0.337 |

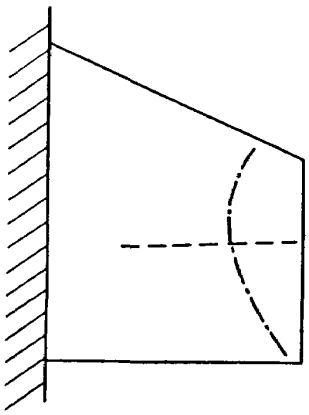

Mode Node Line
1st: At Root,
2nd: ------,
3rd: -·-·-·-

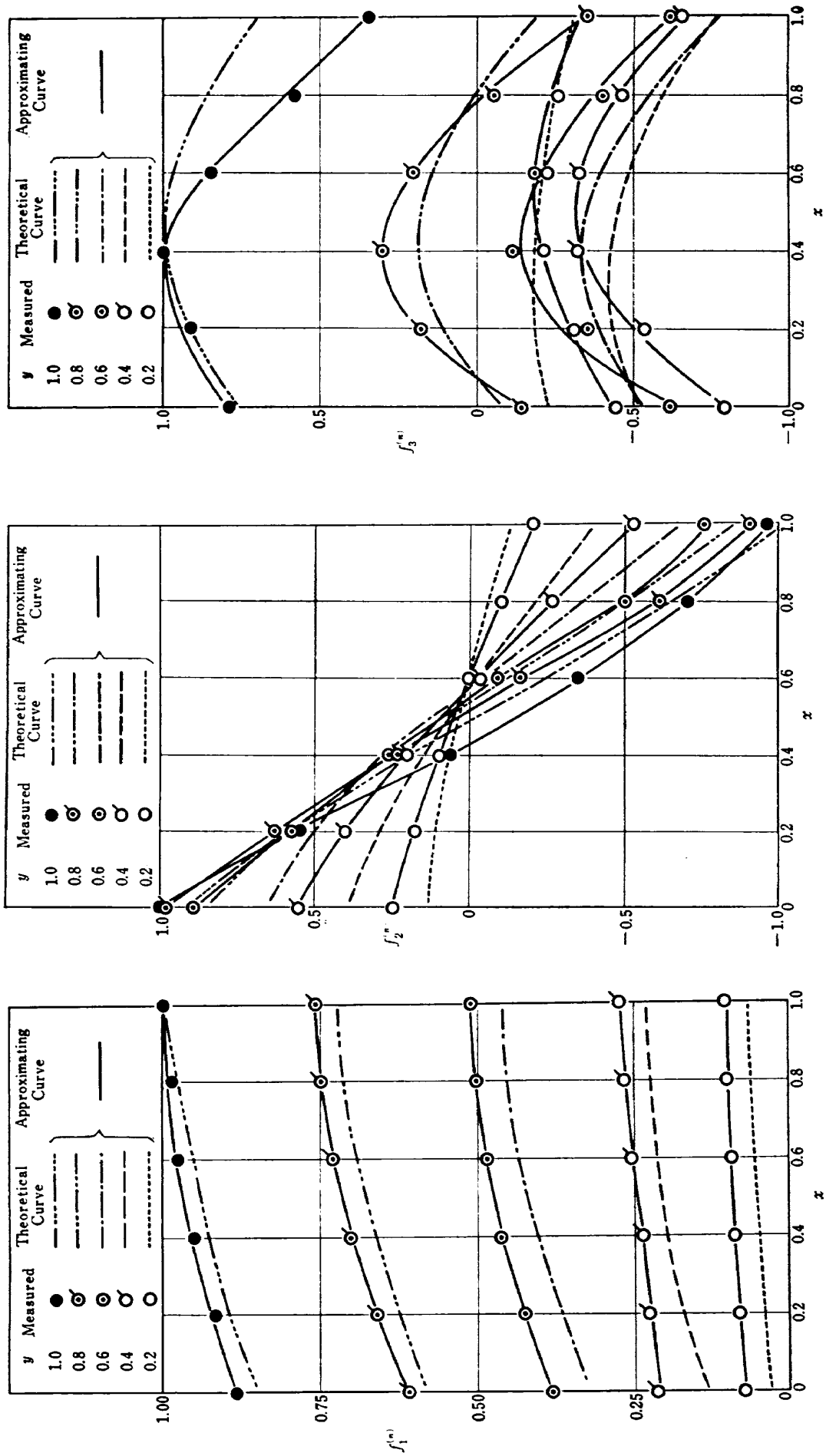


(a) 1st Mode (b) 2nd Mode (c) 3rd Mode

**Fig. 3 Comparison Among Measured and Theoretical Chord Defrection Mode Shapes and Their Polynominal Approximations for the First Three Natural Modes at Various Span Stations.**

of "Model-90" were measured by a bouncing sound technique of reference 7 for use in flutter analysis and presented in table 2 along with natural vibration node lines. In figures 3(a) through 3(c), the measured mode shapes are compared with the corresponding calculated mode shapes by the use of theory of reference 10.

## TEST PROCEDURE

The tests were made at constant Mach numbers with stagnation pressure being increased during the operation of wind tunnel until flutter was encountered or until the tunnel limits were reached.

The testa were originally intended to be conducted at Mach numbers from 1.5 to 4.0 with interval of Mach number of 0.25, but the measured Mach numbers were slightly different from them. The models were not damaged during flutter tests and could be used for succeeding tests, except only "Model-85" which was broken by stopping-shock in the test section because of mulfunction of wind tunnel control system. It was tried to obtain flutter points with more than one model at the same Mach number in order to ensure the results of the experiment, whenever possible.

Table 3. Experimental and Theoretical Results.

| Model | $M$ | Flutter Conditions | | | | $\frac{b_R\omega_\alpha}{a}\sqrt{\mu}$ | | | $f_{f,ex}/f_{f,th}$ | |
|---|---|---|---|---|---|---|---|---|---|---|
| | | $\rho$ kg·s²/m⁴ | $a$ m/s | $q$ kg/m² | $\mu$ | Exp. | Theory | | Theory | |
| | | | | | | | P.T. | Q.S.T. | P.T. | Q.S.T. |
| 65* | | | | | | | | | | |
| 70 | 1.527 | 0.0965 | 283.2 | 9012 | 29.556 | 2.200 | 1.752 | 1.999 | 0.906 | 0.902 |
| 72.5 | 1.519 | 0.0864 | 283.6 | 8021 | 31.890 | 2.147 | 1.736 | 2.029 | 0.919 | 0.924 |
| | 1.780 | 0.0750 | 269.6 | 8639 | 36.734 | 2.426 | 1.909 | 2.106 | 0.903 | 0.908 |
| 75 | 1.771 | 0.0718 | 268.3 | 8111 | 37.096 | 2.419 | 1.907 | 2.095 | 0.904 | 0.904 |
| | 2.037 | 0.0687 | 253.7 | 9177 | 38.817 | 2.617 | 2.056 | 2.200 | 0.924 | 0.924 |
| 77.5 | 2.037 | 0.0567 | 253.9 | 7588 | 45.466 | 2.599 | 2.081 | 2.222 | 0.947 | 0.952 |
| | 2.282 | 0.0555 | 240.8 | 8376 | 46.481 | 2.769 | 2.209 | 2.341 | 0.957 | 0.963 |
| 80 | 2.528 | 0.0541 | 227.9 | 8977 | 46.256 | 2.860 | 2.328 | 2.428 | 0.968 | 0.962 |
| 82.5 | 2.517 | 0.0532 | 228.9 | 8825 | 45.600 | 2.835 | 2.314 | 2.420 | 0.966 | 0.966 |
| | 2.828 | 0.0499 | 213.0 | 9055 | 48.606 | 3.145 | 2.491 | | 0.950 | |
| 85 | 3.064 | 0.0415 | 201.7 | 7929 | 56.771 | 3.249 | 2.613 | | 0.991 | |
| 87.5 | 3.071 | 0.0391 | 202.8 | 7596 | 58.472 | 3.291 | 2.599 | | 0.977 | |
| | 3.280 | 0.0432 | 194.1 | 8765 | 52.916 | 3.273 | 2.672 | | 0.973 | |
| | 3.595 | 0.0425 | 181.4 | 9028 | 53.866 | 3.532 | 2.834 | | 0.974 | |
| 90 | 3.583 | 0.0388 | 182.4 | 8282 | 57.438 | 3.483 | 2.833 | | 0.985 | |
| | 3.848 | 0.0383 | 172.7 | 8460 | 58.155 | 3.702 | 2.938 | | 0.985 | |
| | 4.140 | 0.0344 | 163.7 | 7909 | 64.718 | 4.121 | 3.082 | | 0.977 | |
| 95* | | | | | | | | | | |
| 100* | | | | | | | | | | |

* No flutter was obtained.

P.T.: Piston Theory
Q.S.T.: Quasi-Steady Second-Order Theory

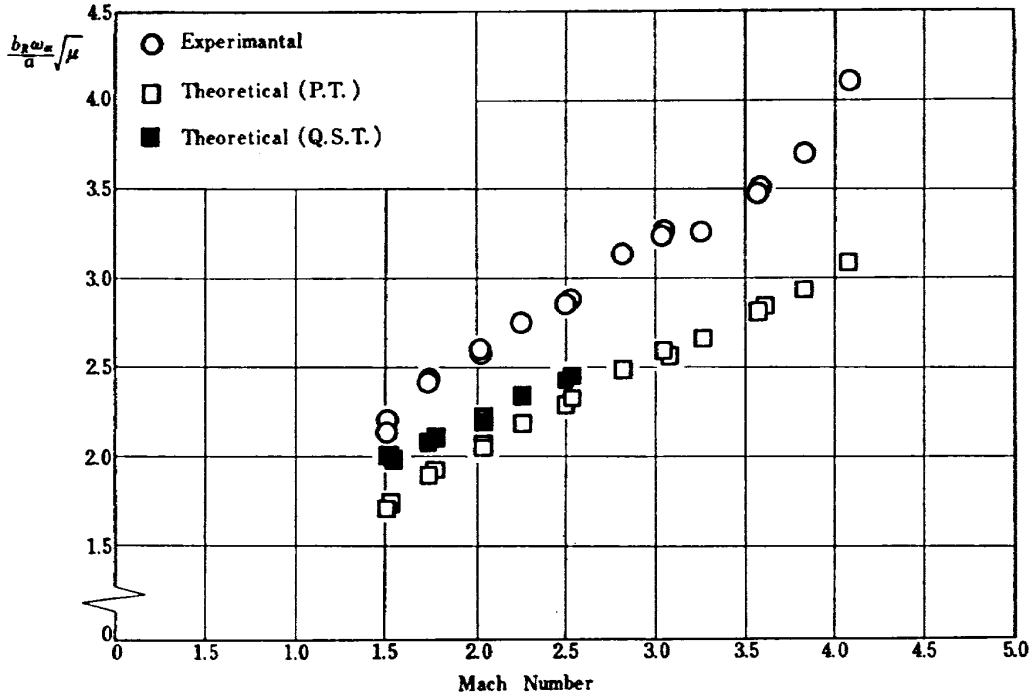


**Fig. 4 Experimental and Theoretical Variaton of Stiffness-Altitude Parameter with Mach Number.**

## RESULTS AND DISCUSSION

The experimental and theoretical results are listed in table 3 and are shown in figure 4 in which both an experimental and a theoretical stiffness-altitude parameter $\frac{b_R\omega_\alpha}{a}\sqrt{\mu}$ required for flutter are plotted as a function of Mach number. The $\omega_\alpha$ is the second natural frequency $f_2$ which is predominantly torsional for models. The mass-density parameter $\mu$ is the ratio of the mass of the wing to the mass of a volume of air enclosing the wing. The volume is that of a truncated cone with the two ends parallel to the airstream with diameter equal to the root and tip chords. The air density $\rho$, which is used in the computation of $\mu$, is the test section density at flutter. The flutter region is below the curves and the non-flutter region is above the curves.

The theoretical flutter boundaries shown in figure 4 were calculated with the use of theory of reference 6, which is described in Appendix, employing aerodynamic forces obtained from piston theory[11] for the full range of Mach number experimented and from quasi-steady second-order theory[12] for Mach number under 2.5, and using the first three natural vibration modes measured. When the theoretical and experimental flutter boundaries are compared, it is seen that the shape of the boundaries agrees well. And, the agreement between the experimental and theoretical flutter boundaries is fairly good at all Mach numbers, that is, the values of the theoretical stiffness-altitude parameters by piston theory are lower than those of the experimental stiffness-altitude parameters by about 20%, and the stiffness-altitude parameters calculated by quasi-steady second-order theory followed the experimental trend of stiffness-altitude parameters more closely at the lower supersonic Mach numbers with decreasing Mach number. Furthermore, since the lifting-pressure expression associated with piston theory and with quasi-steady second-order theory (as shown in equations (1) and (2) in Appendix) approaches each other as Mach numbers approach infinity, the speeds indicated by the two theories also

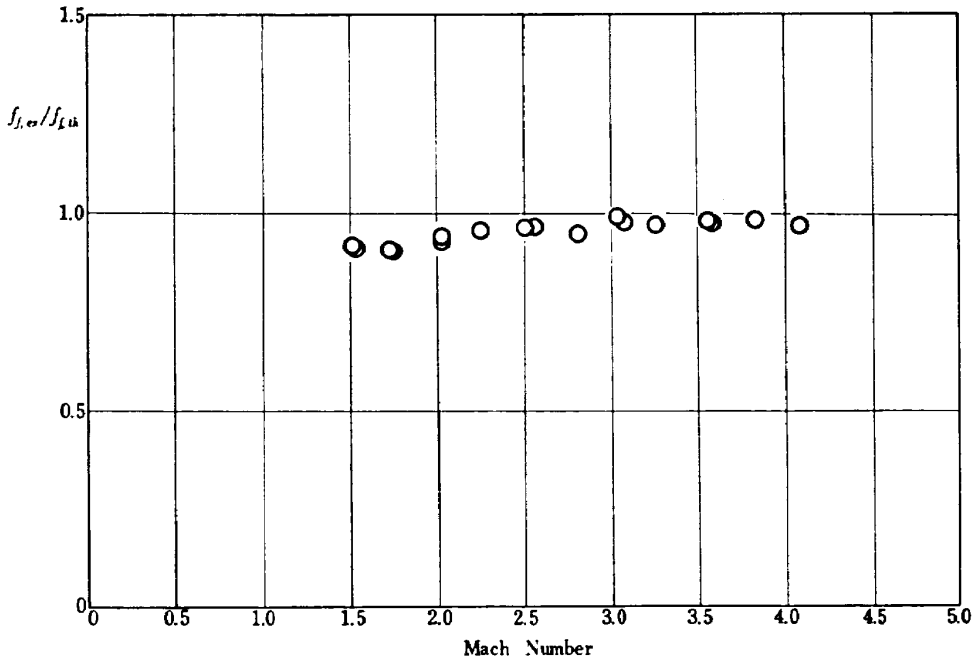


Fig. 5 Variation of the Ratio of Experimental to Theoretical Flutter Frequency with Mach Number.

approach each other as Mach number increases up to around 2.5.

The both theories were unconservative for the configuration of the models investigated and the range of Mach numbers experimented.

Figure 5 shows the variation of the ratio of theoretical flutter frequency calculated by piston theory to experimental flutter frequency with Mach numbers, and the ratio increases with the increase of Mach number. The agreement between the theoretical and experimental flutter frequencies was better than that between flutter boundaries. There was little difference between the flutter frequencies obtained from piston theory and from quasi-steady second-order theory.

## CONCLUSIONS

The results of an investigation conducted in the N.A.L. 1 m×1 m supersonic blow-down wind tunnel of a low aspect-ratio flat-plate surfaces indicated the following conclusions;

1. Both piston theory and quasi-steady second-order theory were unconservative for the configuration of the models investigated and the range of Mach numbers experimented.

2. The agreement between the experimental and theoretical flutter boundaries is fairly good at all Mach numbers experimented.

3. At the lower supersonic Mach numbers, the stiffness-altitude parameters calculated by quasi-steady second-order theory followed the experimental trend of stiffness-altitude parameters more closely with the decrease of Mach number than by piston theory.

4. The agreement between the experimental and theoretical flutter frequencies was good, and there was little defference between the flutter frequencies obtained from piston theory and from quasi-steady second-order theory.

The wind tunnel tests of this investigation were conducted with the cooperation of the staff of Sections of Blow-Down Supersonic Wind Tunnel Control and Measurement, the Second Aerodynamics Division.

## APPENDIX

*Aerodynamic Forces*

The aerodynamic forces are calculated by two procedures: (a) piston theory and (b) a quasi-steady method based on second-order two-dimensional theory.

The second-order piston theory relation and the quasi-steady second-order theory relation between pressure and down-wash, as given in reference 11 and in reference 12 respectively, are

$$p-p_\infty=\rho a^2\left[\frac{w}{a}+\frac{\gamma+1}{4}\left(\frac{w}{a}\right)^2\right]\text{(Piston Theory)} \quad (1)$$

and

$$p-p_\infty=\rho a^2\left(\frac{M}{\beta}\right)\left[\frac{w}{a}+\frac{M^4(\gamma+1)-4\beta^2}{4\beta^3 M}\left(\frac{w}{a}\right)^2\right]$$

(Quasi-Steady Second-Order Theory) (2)

*Flutter Determinant*

The equation of motion at flutter for piston theory aerodynamics are

$$M_i\left[\left(\frac{\omega_i}{\omega}\right)^2 X-1\right]\bar{\xi}_i+\frac{2\rho}{M}\left[\left(\frac{b_R}{k_R}\right)^2(A_{ij}+GC_{ij})+i\left(\frac{b_R}{k_R}\right)\left(B_{ij}+GD_{ij}\right)\right]\bar{\xi}_j=0$$

(subscript $i=1, 2, \ldots$ I) (3)

where

$$\left.\begin{aligned}\xi(t)&=\bar{\xi}e^{i\omega t}\\ X&=\left(\frac{\omega_1}{\omega}\right)^2(1+ig)\\ k_R&=b_R\frac{\omega}{V}\end{aligned}\right\} \quad (4)$$

The subscript $R$ refers to any convenient reference station.

The requirement for a nontrivial solution to equation (3) is that the determinant of coefficients of $\bar{\xi}_i$ must vanish. Thus, in matrix notation,

$$\left|\frac{M}{2\rho}\left[M_i\left\{X\left(\frac{\omega_i}{\omega_1}\right)^2-1\right\}\right]+\left(\frac{b_R}{k_R}\right)^2\left[A_{ij}+GC_{ij}\right]+i\left(\frac{b_R}{k_R}\right)\left[B_{ij}+GD_{ij}\right]\right|=0 \quad (5)$$

where $G=M\frac{\gamma+1}{2}$, $[\ \ ]$ indicates a square matrix, and $\left[\ \ \right]$ indicates a diagonal matrix.

$$\left.\begin{aligned}A_{ij}&=\iint_S\left[\frac{\partial f_j(x',y')}{\partial x'}\right]\left[f_i(x',y')\right]dx'dy'\\ B_{ij}&=\iint_S\left[f_j(x',y')\right]\left[f_i(x',y')\right]dx'dy'\\ C_{ij}&=\iint_S\left[\frac{\partial}{\partial x'}Z(x',y')\right]\left[\frac{\partial f_j(x',y')}{\partial x'}\right]\left[f_i(x',y')\right]dx'dy'\\ D_{ij}&=\iint_S\left[\frac{\partial}{\partial x'}Z(x',y')\right]\left[f_j(x',y')\right]\left[f_i(x',y')\right]dx'dy'\end{aligned}\right\} \quad (6)$$

$$M_i=\iint_S m(x',y')\left[f_i(x',y')\right]\left[f_j(x',y')\right]dx'dy' \quad (7)$$

If the quasi-steady pressures given by equation (2) had been used, flutter determinant would be the same except that $\beta$ would replace $M$ and the factor $G$ would be replaced by $\bar{G}=\frac{M^4(\gamma+1)-4\beta^2}{2\beta^3}$.

*Representation of Wing Deflections and Generalized Mass*

A numerical evaluation of the surface integrals defined by equations (6) and (7) is accomplished by approximating the wing characteristics at a limited number of spanwise stations, performing the chordwise integrations, and then summing spanwise. In order to use this method, the wing is divided into $N$ spanwise stations parallel to the airstream. At each of these stations, the chordwise distribution of displacement of mode $i$ is approximated by a polynomial of degree $P$ over the chord, as shown in figures 3(a) through 3(c) for the respective mode. That is, the total deflection at station $n$ in mode $i$ is given by

$$f_i^{(n)}(x)=\sum_{p=0}^{P}(a_i^{(n)})_p x^p \quad (0\leqq x\leqq 1.0) \quad (8)$$

where $x$ is a nondimensional streamwise coordinate having the value zero at the leading edge and 1.0 at the trailing edge. The coefficient $(a_i^{(n)})_p$ is constant.

The surface integrals of equation (6) can be written in terms of the deflection polynomials by substituting equation (8). The spanwise coordinate becomes $y$, which is zero

at the wing root and unity at the tip. Thus, equation (6) become

$$\left.\begin{aligned}
A_{ij}&=l\int_0^1\left\{\int_0^1\left[\sum_{p=0}^{P_j}\sum_{r=0}^{P_i}p\left(a_j^{(n)}\right)_p\left(a_i^{(n)}\right)_r x^{p+r-1}\right]dx\right\}dy\\
B_{ij}&=2b_Rl\int_0^1\left(\frac{b}{b_R}\right)\left\{\int_0^1\left[\sum_{p=0}^{P_j}\sum_{r=0}^{P_i}\left(a_j^{(n)}\right)_p\left(a_i^{(n)}\right)_r x^{p+r}\right]dx\right\}dy\\
C_{ij}&=l\int_0^1\left[\sum_{p=0}^{P_j}\sum_{r=0}^{P_i}p\left(a_j^{(n)}\right)_p\left(a_i^{(n)}\right)_r\left(t^{(n)}{}_{p+r-1}\right)\right]dy\\
D_{ij}&=2b_Rl\int_0^1\frac{b}{b_R}\left[\sum_{p=0}^{P_j}\sum_{r=0}^{P_i}p\left(a_j^{(n)}\right)_p\left(a_i^{(n)}\right)_r\left(t^{(n)}{}_{p+r}\right)\right]dy
\end{aligned}\right\}\quad(9)$$

The $t_\nu^{(n)}$ term appearing in these equations is constant which are determined by airfoil thickness and cross section and is defined by the following equation:

$$t_\nu^{(n)}=\left[\frac{Z^{(n)}(1)}{2b}\right]-\nu\int_0^1 x^{\nu-1}\left[\frac{Z^{(n)}(x)}{2b}\right]dx \qquad (10)$$

where $\nu$ takes on the values of the indices in equation (9). The quantity $Z^{(n)}(x)$ describes the airfoil contour at station $n$ and is taken as positive when measured away from the mean chord.

Since $m(x', y')$ is constant $m_0$ in flat plate surface, the generalized mass $M_i$ defined by equation (7) becomes

$$M_i=2b_Rlm_0\int_0^1\frac{b}{b_R}\int_0^1\left[\sum_{p=0}^{P}(a_i^{(n)})_p x^p\right]^2dxdy \qquad (11)$$

## REFERENCES


1) Tuovila, W. J., and McCarthy, John Locke: Experimental Flutter Results for Cantilever Wing Models at Mach Numbers up to 3.0. NACA RM L55E11, 1955.
2) Runyan, Harry L. and Morgan, Homer G.: Flutter at Very High Speeds. NASA TN D-942, August 1961.
3) Bennett, Robert M., and Yates, E. Carson, Jr.: A Study of Several Factors Affecting the Flutter Characteristics Calculated for Two Swept Wings by Piston Theory and by Quasi-Steady Second-Order Theory and Comparison with Experiments. NASA TN D-1794, May 1963.
4) Hanson, Perry W., and Levey, Gilbert H.: Experimental and Calculated Results of a Flutter Investigation of Some Very Low Aspect-Ratio Flat-Plate Surfaces at Mach Numbers from 0.62 to 3.00. NASA TN D-2038, October 1963.
5) Kuroda, Y., et al.: Single-Stage Solid-Propellent Rocket "NAL-16"—Design and Flight Experiment. NAL TR-115 (To be published).
6) Morgan, Homer G., Huckel, Vera, and Runyan, Harry L.: Procedure for Calculating Flutter at High Supersonic Speed Including Camber Deflections and Com- and Comparison with Experiments. NASA TN-4335, September 1958.
7) Hanson, Perry W., and Tuovila, W. J.: Experimental and Calculated Results of a bration Modes of Some Cantilever-Wing Flutter Models by Using an Acceleration Method. NACA TN 4010, 1957.
8) The Staff of the Second Aerodynamics Div., N.A.L.: On Design and Construction of the 1 m×1 m Supersonic Blow-Down Wind Tunnel. NAL TR-29, October 1962 (In Japanese).
9) Nakai, Eiichi, et al.: A Method of Calculating Mode Shapes and Frequencies of Cantilever Beam with Variable Cross Section. NAL TM-14, March 1963 (In Japanese).
10) Kawai, T., et al.: On the Natural Vibration of Plate-Like Wings. NAL TR-30, September 1962 (In Japanese).
11) Ashley, Holt, and Zartarian, Garahed: Piston Theory—A New Aerodynamic Tool for the Aeroelastician. Jour. Aero. Sci., Vol. 23, No. 12, Dec. 1956, pp. 1109–1118.
12) Van Dyke, Milton D.: A Study of Second-Order Supersonic Flow Theory. NACA Rept. 1081, 1952.

| | | | |
|---|---|---|---|
| TR-114 | Analytical and Simulation Studies on the Height Control System of the Flying Test Bed (I) | Shun TAKEDA & Tadao KAI | Aug. 1966 |
| TR-115 | Single-Stage Solid Propellant Rocket (NAL-16) | Rocket Study Group | Aug. 1966 |
| TR-116 | Design and Construction of the 50 cm Hypersonic Wind Tunnel at National Aerospace Laboratory | Hypersonic Wind Tunnel Construction Group | Sep. 1966 |
| TR-117 | Energy Inequalities for the Difference Solutions of Equations of Elastic Vibration | Hajime MIYOSHI | Oct. 1966 |
| TR-118 | Some Experiments on High Intensity Combustor with Partial Models | Teikichi OTSUKA, Hiroshi FUKUDA & Tetsuro AIBA | Oct. 1966 |
| TR-119 | On the Existence of Discontinuous Solutions of the Cauchy Problem for Quasi-Linear First-Order Equations | Kiyofumi KOJIMA | Oct. 1966 |
| TR-120 | Analytical and Simulation Studies on the Attitude Control System of the Flying Test Bed | Shun .TAKEDA, Yuso HORIKAWA, Toshio OGAWA & Mikihiko MORI | Nov. 1966 |
| TR-121 | Some Circuits for Pulse-Ratio-Modulation and their Modified Circuits | Chikara MURAKAMI | Nov. 1966 |
| TR-122 | Semi-Empirical Theory to Estimate the Airforces Acting on the Two-Dimensional Harmonically Oscillating Wing at High Angle of Attack Where Separation Can Occur | Kozi ISOAGI | Dec. 1966 |
| TR-123 | Design and Experimental Study on Air Jet Nozzles for the Attitude Control of VTOL Aircraft | Naoto TAKIZAWA, Hiroshi NISHIMURA, Hirotoshi FUJIEDA, Yoshikazu TANABE & Akiyoshi SHIBUYA | Dec. 1966 |
| TR-124 | Dynamic Characteristic of FM Multichannel Telemetering System | Keiji NITTA, Yoshio SAKURAI & Ioshitsugu MATSUZAKI | Dec. 1966 |


**TECHNICAL REPORT OF NATIONAL AEROSPACE LABORATORY**
**TR-125T**

# 航空宇宙技術研究所報告 125 号 (欧文)

昭和 42 年 1 月 発行

発行所 航空宇宙技術研究所
東京都調布市深大寺町 1,880
電話武蔵野三鷹(0422)44-9171 (代表)

印刷所 株式会社 東京プレス
東京都板橋区桜川 2 丁目 27 の 12

Published by
NATIONAL AEROSPACE LABORATORY
1,880 Jindaiji, Chōfu, Tokyo
JAPAN